Modeling Natural Steam Cap Formation in High-Enthalpy Geothermal Systems

Samuel Scott

Reykjavik University, Reykjavik, Iceland

Previously at ETH Zurich, Zurich, Switzerland

Keywords

Boiling, steam cap, vapor, two-phase flow, cap rock, permeability

ABSTRACT

Many high-enthalpy geothermal systems develop vapor-rich boiling zones (steam caps) at depths less than 1 km, representing economically-attractive resources. However, the geologic and hydrologic factors that lead to steam cap development are not well understood. Numerical simulations of fluid convection around transiently cooling magmatic intrusions show how a steam cap forms near the base of a low permeability clay cap extending to 0.5 km depth. These zones may form naturally in later stages of system evolution as the strength of fluid upflow decreases as the heat source cools. Broadly, these models reveal how transient changes in heat source geometry and temperature exercise an important control on the thermo-hydraulic structure of magma-driven geothermal systems. Such processes may be masked in natural state simulations that model a steady-state thermal structure in response to fixed boundary conditions (heat and mass input) at the base of the model.

1. Introduction

Many high-enthalpy geothermal systems worldwide develop vapor-dominated boiling zones at <1 km depth (hereafter referred to as ‘steam caps’) overlying liquid-dominated upflows at greater depth. However, while vapor-dominated geothermal systems featuring vertically-extensive vapor-dominated boiling zones extending from the near-surface to depths >1-2 km have received a lot of research attention (White et al., 1971; Truesdell and White, 1973; Pruess and Narasimhan, 1982; Ingebritsen and Sorey, 1988; Raharjo et al., 2016), such systems are relatively rare. Steam caps are far more common, yet in some ways less well understood.

In several exploited high-enthalpy geothermal systems, fluid withdrawal and subsequent pressure decline has led to the development and/or expansion of steam caps, as in Wairakei (Bixley et al., 2009), Svartsengi (Björnsson, 1999), Mahanadong (Menzies et al., 2010) and Tonganon (Dacillo

and Siega, 2005). However, there is also evidence that steam caps were present in the natural, pre-exploitation state of systems such as Tolhuaca (Melosh et al., 2012), Tiwi (Gambill and Beraquit, 1993), Olkaria (Bödvarsson et al., 1987), Ohaaki (Mroczek et al., 2016) and several systems in East Java, Indonesia (Acuna et al., 2008; Bogie et al., 2008; Moore et al., 2008). From an economic perspective, the ability to target local vapor-dominated reservoirs within larger liquid-dominated geothermal systems is extremely advantageous, as the produced fluid is higher enthalpy and less of the discharged fluid must be separated and reinjected. Thus, wells drilled into steam caps contribute substantially to the overall power generation in these systems. However, there are several scientific questions related to the formation of steam caps and their response to production that require better understanding to improve the reliability of these reservoirs for geothermal power generation. While several studies have investigated the response of steam caps to production (Bödvarsson, 1988; Björnsson, 1999; Hanano, 2003; Zarrouk et al., 2007; Pratama and Saptadji, 2015), less attention has been given to the geologic and hydraulic factors that may result in natural shallow vapor-dominated boiling zones.

In this study, I use numerical models of fluid flow around transiently cooling intrusions to explore the formation of steam caps. Shallow, vapor-dominated boiling zones develop at the base of cap rocks during the waning stages of system development, when the magmatic heat source has been cooled by hydrothermal circulation, the over-pressure that drives fluid convection is reduced, and as a result fluid pressures in the boiling zone decrease. The spatial extent (thickness and lateral extent) and enthalpy of steam zones depends on host rock permeability. While it has long been known that steam cap formation can be induced by fluid withdrawal, this study highlights how such zones can develop in natural, magma-driven geothermal systems.

2. Methodology and Model Set-Up

The simulations are performed with the Complex Systems Modeling Platform (CSMP++), which uses a continuum porous media approach and a Control Volume-Finite Element Method to solve the governing equations of multi-phase mass and energy conservation with a pressure-enthalpy-based formulation. The numerical scheme has been described in detail by Weis et al. (2014) and benchmarked with other well-established codes, including HYDROTHERM (Hayba and Ingebritsen, 1997) and TOUGH2 (Pruess et al., 2007). The equation of state of Haar et al. (1984) is used to determine phase relations and fluid properties of pure H_2O. A linear relative permeability model is used with a vapor residual saturation of zero and liquid residual saturation of 0.3 (Hayba and Ingebritsen, 1997; Weis et al., 2014). Thermal equilibrium between the rock and fluid at a given node in the mesh and at each time step is ensured by iterating temperature at a constant pressure and redistributing the total enthalpy between rock and fluid according to their thermodynamic properties until they each have the same temperature.

An example model set-up is shown in Figure 1. A sill-shaped intrusion with horizontal and vertical axis lengths of 4 km and 1 km, respectively, is emplaced at 2.5 km depth (centered at 3 km depth). Initially, the porous medium is saturated with water and thermally equilibrates with a basal heat flux of 0.15 W m^{-2}. The initial pressure distribution is hydrostatic, assuming the water table coincides with the ground surface and that the topography is flat. The top boundary is fixed at atmospheric pressure, and features a mixed energy boundary condition. In elements where volume flux is upward, fluids vent at temperatures of the ascending hydrothermal fluids; elements where the volume flux is downward take in fluid at a temperature of 10 °C, simulating

the effect of recharge of cold meteoric water sufficient to maintain a stable elevation of the water table. As the computational domain is 5 km and 15 km in vertical and horizontal extent, respectively, the boundaries other than the top boundary are placed sufficiently far from the heat source that the no-flow condition they impose does not affect convection near the intrusion.

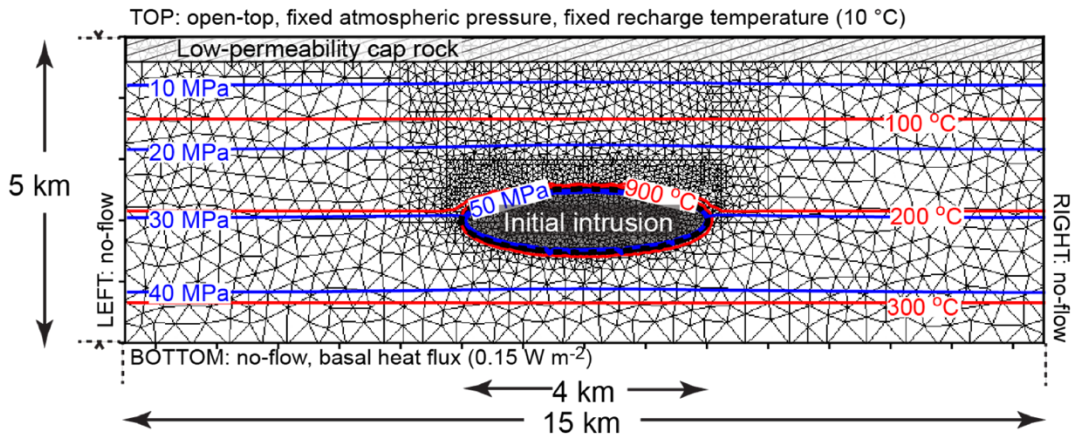

Figure 1: Model set-up and finite element discretization. Initial temperature and pressure distribution is shown with red and blue contours, respectively. The boundaries of the initial intrusion are shown with dashed black lines. The location of the low permeability cap rock is shown hatching.

At the onset of simulation time, fluid within the pore space of the intrusion is set to a temperature of 900 °C and lithostatic pressure, describing an instantaneous intrusion of magma into the upper crust. The effect of latent heat of crystallization is taken into consideration with a temperature-dependent rock heat capacity, which doubles from 880 J kg^{-1} °C at temperatures below 650 °C to 1760 J kg^{-1} °C at temperatures greater than 700 °C. To represent the transition from conduction- to advection-dominated heat transfer around the intrusion, the permeability of the intrusion and host rock is temperature-dependent according to the formulation first introduced by Hayba and Ingebritsen (1997), in which permeability decreases log-linearly above a selected temperature from the background, host-rock permeability to a value of 10^{-22} m^2. The temperature at which permeability starts to decrease is interpreted as the onset of the brittle-ductile transition, and is set to 450 °C based on experimental evidence for basaltic rocks (Violay et al., 2012).

The model is set up to investigate the impact of host rock permeability and the thickness of low permeability cap rock on the formation of shallow vapor zones. The system-scale permeability of geothermal systems is generally estimated to range from approximately 10^{-14} m^2 to 10^{-15} m^2 (Björnsson and Bödvarsson, 1990), and we vary host rock permeability between these values. We set cap rock permeability to 10^{-16} m^2 based on previous modeling studies that have shown clay cap permeability must be less than or equal to this value to support the development of vapor-dominated boiling zones (Ingebritsen and Sorey, 1988; Raharjo et al., 2016). A permeability of 10^{-14} m^2 is hereafter referred to as high permeability, 10^{-15} m^2 intermediate, and 10^{-16} m^2 low, because heat transfer is conduction-dominated below this value (Ingebritsen et al., 2006). The thickness of the cap rock is set to 0.5 km based on field evidence (see studies cited in the introduction) and the thickness of the cap rock is constant over the entire width of the

domain. Clearly, this is a simplification as cap rocks have variable depth and lateral extent in real systems, and develop dynamically in response to changing temperatures and fluid chemistry. Investigating the effect of the lateral width of the cap rock, dynamic changes in the width and thickness of the cap rock, or other lateral permeability variations is beyond the scope of the present study.

3. Results

Simulation results are presented following the framework of Scott et al. (2016), which divides the temporal evolution of magma-driven geothermal systems into three stages: (i): the incipient stage, when ascending upflow plumes haven't reached the surface; (ii.) the main stage, when upflow plumes extend from the surface to the depth of the heat source; and (iii.) the waning stage, after continued hydrothermal circulation cools the entire heat source below the brittle-ductile transition temperature (450 °C for these simulations) and temperatures decrease at depth while boiling persists near the surface.

3.1 Temporal evolution and spatial extent of steam caps

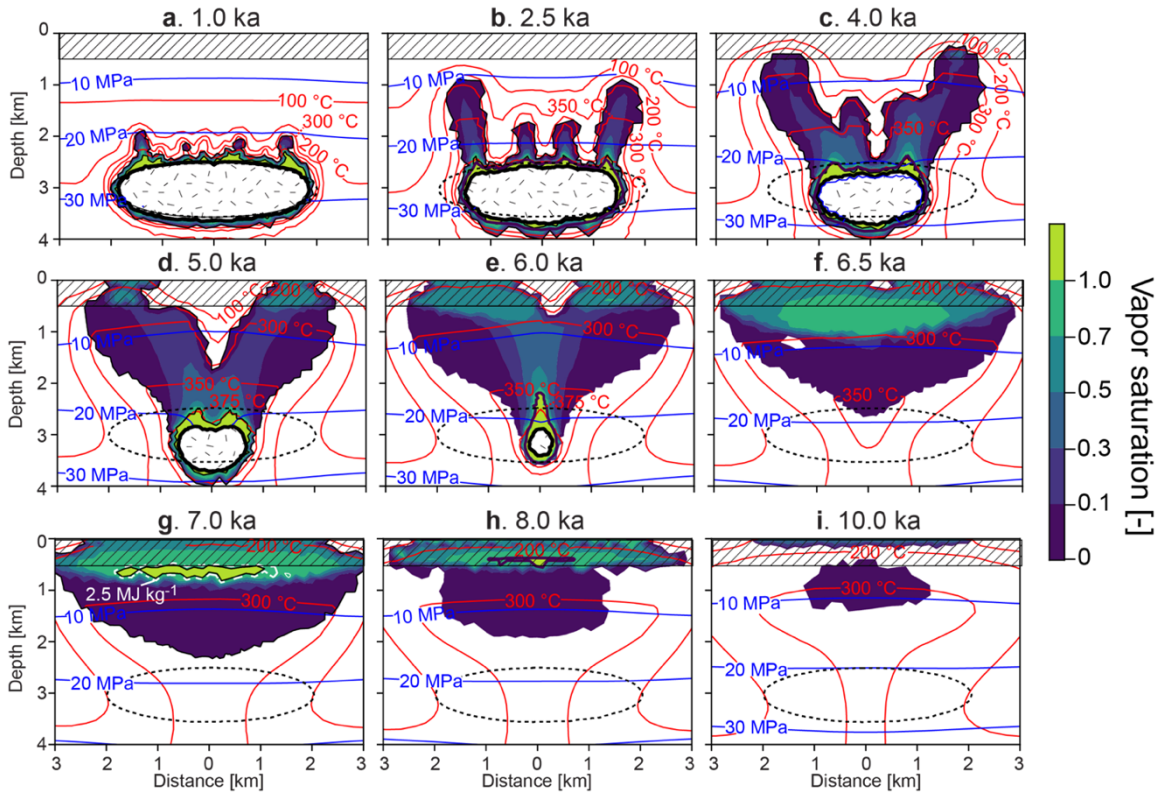

Figure 2: Evolution of thermal structure for systems with intermediate host rock permeability and a low permeability cap rock in upper 0.5 km. Snapshots taken at a given time and show vapor saturation, temperature isotherms in red and isobars in blue. The geometry of the initial intrusion is shown with dashed lines and the location of the impermeable intrusion at the given time is shown with stippled filling. The cap rock is showed with hatching.

Shallow vapor zones form during the later stages of system evolution near the interface between the reservoir rock and a low permeability cap rock. Figure 2 shows results for a system with intermediate permeability host rock and a low permeability cap rock that extends from the surface to 0.5 depth. During the incipient stage, boiling plumes with vapor saturation <0.3 ascend most rapidly above the margins of the intrusion (Fig. 2a-c). The plumes reach the surface ca. 4 ka after intrusion emplacement, and the system develops a vertically-extensive boiling zone extending from the surface to close to the depth of the intrusion. By this time, the area of the impermeable intrusion (as defined by permeability $<10^{-16}$ m^2) is significantly less than from the initial size (black dashed line) due to hydrothermal cooling. During the main stage, the maximum vapor saturation between 1-2 km depth (0.3-0.5) are found directly above the center of the intrusion, and somewhat higher vapor saturations are found (0.5-0.7) in the upper 1 km and directly above the supercritical zone surrounding the intrusion (Fig. 2d-e). After hydrothermal circulation has cooled the entire intrusion to 450 °C (Fig. 2f), indicating the onset of the waning stage, a ~2 km wide, ~0.5 km thick steam cap with vapor saturation 0.7-1 develops in the upper km of the system at ~250 °C. Subsequently, the area with vapor saturations of 0.7-1 expands laterally, and a ~0.2 km thick single-phase vapor zone with an enthalpy >2.5 MJ kg^{-1} (white dashed line) develops near the base of the cap rock (Fig. 2g). Later in the waning stage, the vapor zone narrows and thins out as the system cools slowly, and eventually develops into a zone of liquid underlain by a boiling zone with low vapor saturations (Fig. 2h-i).

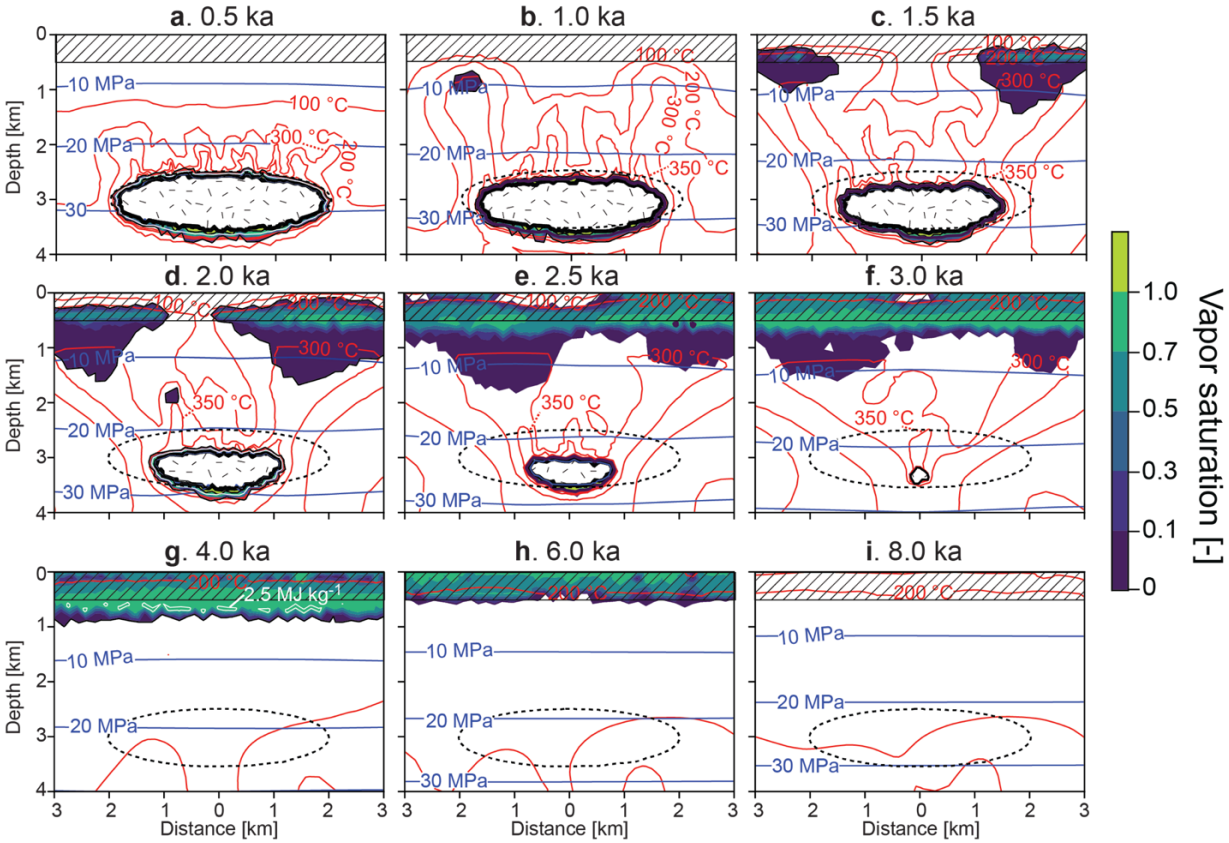

Figure 3: Evolution of thermal structure for systems with high host rock permeability and a low permeability cap rock in upper 0.5 km. Color scheme same as Figure 2.

Thinner steam caps with lower temperatures and enthalpies develop in systems with high host rock permeability and a low permeability cap rock. Figure 3 shows results for system with high host rock permeability and a cap rock extending to 0.5 km depth. During the incipient stage, liquid upflow plumes develop above the intrusion (Fig. 3a). Boiling zones with low vapor saturations (<0.3) form and spread out near the base of the cap rock after 1 ka of system development (Fig. 3b-c). The isotherms are nearly horizontal within the low permeability cap rock, indicating that the boiling zone progresses relatively slowly towards the surface in the upper 0.5 km of the system. The vapor saturation of boiling zones in the upper km of the system become more vapor rich as the intrusion shrinks, as 0.1-0.2 km thick zones with vapor volumetric saturation of 0.7-1.0 develop directly beneath the base of the clay cap (Fig. 3d-f). This zone becomes thicker (up to ~0.4 km) and expands laterally during the waning stage (Fig. 3g), and spans a width greater than the initial width of the intrusion. However, fluid enthalpies >2.5 MJ kg^{-1} only develop within scattered zones that are <0.1 km thick zone below the base of the cap rock (Fig. 3g). Later in the waning stage, the boiling zone confined to the cap rock develops lower vapor saturations (Fig. 3h), and eventually transforms into single-phase liquid (Fig. 3i).

3.2 Fluid flow patterns during steam cap formation

Shallow steam caps develop above a narrow zone of liquid downflow. Figure 4 shows the temporal evolution of vertical fluid mass fluxes for a system with intermediate host rock permeability (Fig. 4a), soon after the intrusion has been cooled and a steam cap is present (Fig. 4b), and further into the waning stage (Fig. 4c). When the hot, impermeable intrusion is still present at depth (Fig. 4a), intensive fluid circulation close to the intrusion results in a strong upflow near 2.5 km depth. After the intrusion is cooled (Fig. 4c), the area with high fluid mass fluxes (>10^{-5} kg m^{-2} s^{-1}) below 2.5 km depth becomes smaller. There is a 0.1-0.2 km thick zone of liquid downflow below the cap rock that spans the center boiling zone beneath the cap rock, and in the center is overlain by a steam cap wedged between the cap rock and the liquid downflow zone. Vertical fluid mass fluxes at depth are further reduced as the waning stage progresses, and the steam cap as well as the zone of liquid downflow between 0.5-1 km depth disappears (Fig. 4c).

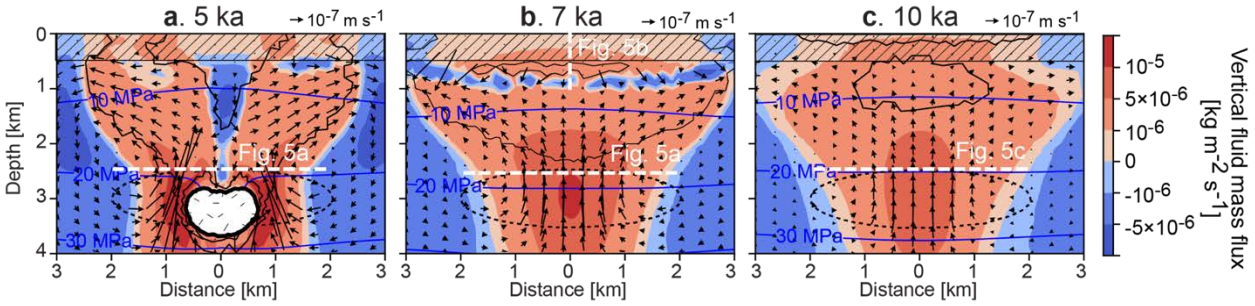

Figure 4: Evolution of fluid mass fluxes in system with intermediate host rock permeability and a low permeability cap rock in upper 0.5 km. Liquid flow vectors are shown in black. Otherwise, color scheme is same as in Figure 2. Location of horizontal and vertical profiles across which vertical fluid mass flux and fluid pressure are plotted in Figure 5a and 5b, respectively, are shown with white dashed lines. Compare this figure with Figure 2.

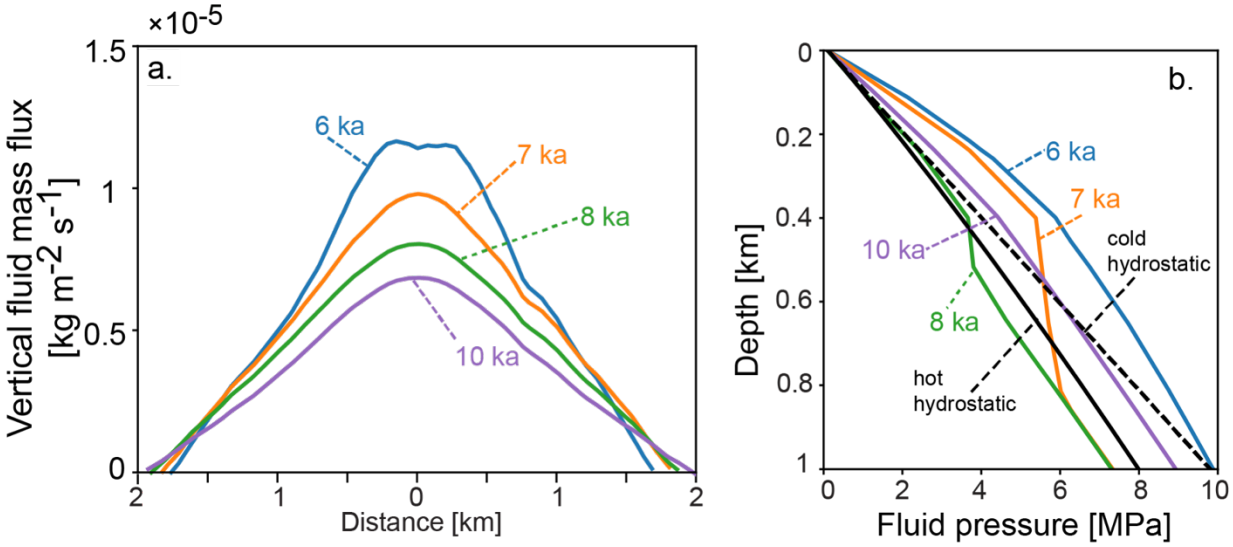

Figure 5: Evolution of fluid mass fluxes and fluid pressures in system with intermediate host rock permeability and a low permeability cap rock in upper 0.5 km. (a) Vertical fluid mass flux across a 4 km wide profile spanning the base of the upflow zone (see Figure 4). (b) Fluid pressure to 1 km depth across a profile in the center of the model (see Figure 4).

Steam caps develop during the beginning of the waning stages of system evolution, after the strength of the upflow is reduced due to the cooling of the intrusion. This can be seen clearly in Figure 5a, which plots how vertical fluid mass fluxes develop with time along a horizontal profile at 2.5 km depth, close to the top of intrusion. Vertical mass fluxes are nearly symmetrical about the center of the model (center of the intrusion), decreasing rapidly between 6-8 ka and more slowly between 8-10 ka. The reduction in the strength of the upflow and magnitude of vertical mass fluxes causes changes in the dynamic (i.e. supra-hydrostatic) pressure gradient which drives fluid convection and the development of the steam cap, as can be seen in Figure 5b, which plots vertical pressure profiles over the center of the model between 6-10 ka (colored lines), and compares them with calculated hydrostatic pressure profiles for cold liquid (dashed line) and vapor-saturated liquid (solid black line). At 6 ka, the vertical pressure gradient significantly exceeds hot hydrostatic due to the influence of the shallow intrusion driving convection. After the intrusion is cooled the vertical pressure gradient is dramatically reduced, and a vapor-static pressure profile develops between 0.4-0.8 km at 7 ka, indicating the development of steam cap. The thickness of the vapor-static pressure profile decreases to 0.1 km by 8 ka. Due to the zone with vapor-static pressures, the pressure beneath the steam cap are less than the hot hydrostatic pressure. However, after 10 ka the steam cap is no longer present and the vertical fluid pressure gradient is about 10% greater than the hot hydrostatic pressure gradient.

4. Discussion

The models show that steam caps form near the base of low permeability cap rocks. This is consistent with previous studies identifying low permeability barriers as necessary to restrict vapor loss to the surface and stabilize overlying liquid condensate above an underlying vapor-dominated region (White et al., 1971; Schubert and Straus, 1980; Straus and Schubert, 1981; Ingebritsen and Sorey, 1988; Allis, 2000; Raharjo et al., 2016). In contrast to some previous

studies, these simulations show that the low permeability barrier need not extend laterally around the steam cap and isolate it from surrounding liquid. Figure 4a-b shows that higher pressures in the center of the upflow compared to the sides of the upflow cause ascending liquid to preferentially flow away from the center of the upflow during ascent. The process of lateral liquid flow at the base of the cap rock is commonly referred to as outflow. Thus, horizontal pressure gradients induced by convection are sufficient to prevent inflow (or 'flooding') of the lower pressure vapor zone by surrounding liquid. However, this is only true if there is sufficient dynamic vertical pressure gradient associated with fluid convection.

This study shows that the size and enthalpy of the steam cap depend on the permeability of underlying reservoir rock, with thicker and higher enthalpy resources developing in intermediate permeability rock, and laterally more extensive and lower enthalpy resources developing in high permeability rock. Permeability controls how rapidly fluid pressure changes resulting from fluid density decrease at high temperature dissipates in the rock medium, resulting from, for example, fluid density decreases due to temperature. In high permeability rocks, the fluid pressure changes are smaller (see flatter isobars in Figure 3 compared to Figure 2). This means that boiling fluid of a given enthalpy and at a given depth will undergo lower magnitude pressure changes due to transient changes in system structure (i.e., the strength of the upflow), meaning that less vapor will be generated by boiling of this fluid.

The models show that a narrow (0.1-0.2 km thick) liquid downflow zone develop directly below the steam cap. While relatively small liquid downflow zones can develop in boiling zones beneath the cap rock when part of the intrusive heat source is still hot (Fig. 4a), they expand vertically and laterally after the intrusion has been completely cooled by hydrothermal circulation (Fig. 4b). While vapor-liquid counterflow (a ‘heat pipe’) has long been known to be a feature of vapor-dominated boiling zones (Straus and Schubert, 1979), these simulations suggest that the zone of intensive liquid downflow is spatially segregated beneath the steam cap, where liquid saturations are still high (<0.1, compare Figure 4b and Figure 2g). Liquid downflow is a result of a decrease in the vertical dynamic pressure gradient beneath the steam zone; the buoyancy forces are no longer sufficient to cause the dense liquid to ascend. This greatly enriches the vapor content of the overlying boiling zone.

While it has long been known that steam caps may develop in response to fluid extraction and subsequent reservoir pressure decrease, these simulations suggest that transient changes in the strength of the upflow could result in the formation of natural steam zones. The transient changes in upflow strength result from the progressive cooling of an initially high-temperature, impermeable intrusion by hydrothermal fluid circulation until temperatures at depth are lower than the temperatures in the overlying geothermal system. For the intrusion geometry considered in this study, cooling of the heat source occurs over timescales of ca. 3-5 ka (depending on permeability), and the steam caps may persist for thousands of years after the heat source is cooled. As evidenced by the formation of shallow vapor zones induced by fluid withdrawal over timescales of years to decades (Bödvarsson, 1988; Björnsson, 1999), the vapor fraction of boiling zones is quite sensitive to pressure decrease. Natural sources of pressure decrease sufficient to transform liquid-dominated boiling zones to vapor-dominated boiling zones could be induced by sudden discharge of fluid through surface vents (Pruess, 1985; Shook, 1995) or decrease in the mass influx of high-enthalpy fluid at the base of the upflow (Ingebritsen and

Sorey, 1988) potentially due to sealing of fractures by mineral deposition (Moore et al., 2000; Scott and Driesner, 2019) or decreasing discharge of magmatic vapor (Moore et al., 2008).

4. Conclusion

Simulations of fluid convection around a transiently cooling intrusion show how natural steam caps may form at the base of the low permeability cap rock at the later stages of system evolution. The permeability of host reservoir rock controls the geometry and enthalpy of steam zones. The steam caps may develop naturally in response to fluid pressure changes resulting from cooling of the heat source and decrease in the strength of fluid upflow.

Further simulations are needed to consider the effects of different relative permeability functions, capillary pressure relations, more complicated cap rock geometries (for example, limited horizontal extent and deepening of the cap rock on the margins of the upflow). In addition, there is not yet a way to model the dynamic development of a cap rock in response to alteration of primary minerals to clays. However, these models reveal how transient changes in heat source geometry and temperature exercise an important control on the thermo-hydraulic structure of magma-driven geothermal systems. Such processes may be masked by the common approach taken in natural state simulations, to model a steady-state thermal structure in response to fixed boundary conditions (heat and mass input) at the base of the model.

Acknowledgement

The simulations were performed during the authors PhD at ETH Zurich between 2012-2016.

REFERENCES

Acuña, J. A., Stimac, J., Sirad-Azwar, L. and Pasikki, R. G. “Reservoir management at Awibengkok geothermal field, West Java, Indonesia.” *Geothermics*, 37, (2008), 332–346.

Bixley, P. F., Clotworthy, A.W. and Mannington, W.I. “Evolution of the Wairakei geothermal reservoir during 50 years of production.” *Geothermics* **38**, (2009), 145–154.

Björnsson, G. “Predicting Future Performance of a Shallow Steam-Zone in the Svartsengi Geothermal Field, Iceland.” *Proceedings: 24th Workshop on Geothermal Reservoir Engineering*, Stanford University, Stanford, CA (1999).

Bödvarsson, G.S., Pruess, K., Stefansson, V., Björnsson, S. and Ojiambo, S.B. “East Olkaria Geothermal Field, Kenya: 1. History match with production and pressure decline data.” *Journal of Geophysical Research*, 92, (1987), 521–539.

Bödvarsson, G.S. “Model Predictions of the Svartsengi Reservoir, Iceland.” *Water Resources Research*, 24, (1988), 1740–1746.

Bogie, I., Kusumah, Y. I. and Wisnandary, M. C. “Overview of the Wayang Windu geothermal field, West Java, Indonesia.” *Geothermics*, 37, (2008) 347–365.

Dacillo, D.B. and Siega, F.L. “Geochemical Assessment on the Sustainability of the Deep Geothermal Resource of Tongonan Geothermal Field (Leyte, Philippines)” *Proceedings World Geothermal Congress*, (2005)

Gambill, D.T. and Beraquit, D.B. “Development history of the Tiwi geothermal field, Philippines.” *Geothermics*, 22, (1993), 403–416.

Haar L. “*NBS/NRC steam tables*”, CRC Press, (1984)

Hanano, M. “Sustainable steam production in the Matsukawa geothermal field, Japan.” *Geothermics*, 32, (2003), 311–324.

Hayba, D.O. and Ingebritsen, S.E. “Multiphase groundwater flow near cooling plutons.” *Journal of Geophysical Research*, 102, (1997), 12235-12252.

Ingebritsen, S. and Sorey, M. “Vapor-Dominated Zones Within Hydrothermal Systems: Evolution and Natural State.”, *Journal of Geophysical Research*, **93**, (1988), 13635-13655.

Melosh, G., Moore, J. and Stacey, R. “Natural Reservoir Evolution in the Tolhuaca Geothermal Field, southern Chile.” *Proceedings 36th Workshop on Geothermal Reservoir Engineering*, Stanford, California, (2012)

Menzies, A., Villaseñor, L., Sunio, E. and Lim, W. “Characteristics of the Matalibong Steam Zone, Tiwi Geothermal Field, Philippines.” *Proceedings World Geothermal Congress*, (2010)

Moore, J. N., Adams, M. C. and Anderson, A. J. “The Fluid Inclusion and Mineralogic Record of the Transition from Liquid- to Vapor-Dominated Conditions in The Geysers Geothermal System”, California.” *Economic Geology*, 95, (2000), 1719–1737.

Moore, J. N., Allis, R. G., Nemcok, M., Powell, T. S., Bruton, C. J., Wannamaker, P. E., Raharjo, I. B. and Norman, D. I. “The evolution of volcano-hosted geothermal systems based on deep wells from Karaha-Telaga Bodas, Indonesia.” *Am. J. Sci.*, 308, (2008), 1–48.

Mroczek, E.K., Milicich, S.D., Bixley, P.F., Sepulveda, F., Bertrand, E.A., Soengkono, S. and Rae, A.J. “Ohaaki geothermal system: Refinement of a conceptual reservoir model.” *Geothermics* 59, (2016), 311–324.

Pratama, H. B. and Saptadji, N.M. “Study of Production-Injection Strategies of Synthetic Geotherml Reservoir Liquid-Dominated Model with Numerical Simulation” *Proceedings 37th New Zealand Geothermal Workshop*, Taupo, New Zealand, (2015)

Pruess, K., Oldenburg, C. and Moridis, G. “TOUGH2 User’s Guide, Version 2.” Berkeley, California. (2012)

Pruess, K. “A Quantitative Model of Vapor Domianted Geothermal Reservoirs as Heat Pipes in Fractured Porous Rock.” *GRC Transactions*, 9, (1985), 353–361.

Pruess, K. and Narasimhan, T.N. “On fluid reserves and the production of superheated steam from fractured, vapor-dominated geothermal reservoirs”. *J. Geophys. Res.*, 87, (1982), 9329-9339.

Raharjo I. B., Allis, R.G. and Chapman, D.S. “Volcano-hosted vapor-dominated geothermal systems in permeability space.” *Geothermics*, 62, (2016), 22–32.

Schubert, G. and Straus, J. M. “Gravitational stability of water over steam in vapor-dominated geothermal systems.” *Journal of Geophysical Research,* 85, (1980), 6505–6512.

Schubert, G. and Straus, J. M. “Steam-Water Counterflow in Porous Media.” *Journal of Geophysical Research,* 84, (1979), 1621–1628.

Scott, S., Driesner, T. and Weis, P. “The thermal structure and temporal evolution of high-enthalpy geothermal systems.” *Geothermics,* 62, (2016), 33–47.

Scott, S. and Driesner, T. “Permeability changes resulting from quartz precipitation and dissolution around upper crustal intrusions.” *Geofluids,* 2018, (2018)

Shook, G. M. “Development of a vapor-dominated reservoir with a “high-temperature” component.” *Geothermics,* 24, (1995), 489–505.

Straus, J. M. and Schubert, G. “One-Dimensional Model of Vapor-Dominated Systems.” *Journal of Geophysical Research,* 86, (1981) 9433–9438.

Truesdell A. H. and White, D. E. “Production of Superheated Steam from Vapor-Dominated Geothermal Reservoirs”, *Geothermics,* 2, (1973), 154–173.

Weis, P., Driesner, T., Coumou, D. and Geiger, S. “Hydrothermal, multiphase convection of H_2O-NaCl fluids from ambient to magmatic temperatures: a new numerical scheme and benchmarks for code comparison.” *Geofluids,* 14, (2014), 347–371.

White D., Muffler L. and Truesdell, A. Vapor-dominated hydrothermal systems compared with hot-water systems. *Econ. Geol.*, 66, (1971), 75–97.

Zarrouk, S., O’Sullivan, M., Croucher, A. and Mannington, W. “Numerical modelling of production from the Poihipi dry steam zone: Wairakei geothermal system”, New Zealand. *Geothermics,* 36, (2007), 289–303.